International Journal of Pharmaceutics 635 (2023) 122667

Contents lists available at ScienceDirect

International Journal of Pharmaceutics

journal homepage: www.elsevier.com/locate/ijpharm

Microfluidics assembly of inhalable liposomal ciprofloxacin characterised by an innovative in vitro pulmonary model

Ye Zhang [a,b], Chun Yuen Jerry Wong [b], Hanieh Gholizadeh [b,c], Annalisa Aluigi [d], Mattia Tiboni [d], Luca Casettari [d], Paul Young [b,e], Daniela Traini [b,c], Ming Li [a], Shaokoon Cheng [a,*], Hui Xin Ong [b,c,*]

[a] School of Engineering, Faculty of Science and Engineering, Macquarie University, Sydney, NSW, Australia
[b] Woolcock Institute of Medical Research, Sydney, NSW, Australia
[c] Macquarie Medical School, Faculty of Medicine, Health and Human Sciences, Macquarie University, Sydney, NSW, Australia
[d] Department of Biomolecular Sciences, University of Urbino Carlo Bo, Piazza del Rinascimento, 6, 61029 Urbino, PU, Italy
[e] Department of Marketing, Macquarie Business School, Macquarie University, Sydney, NSW, Australia

ARTICLE INFO

Keywords:
Ciprofloxacin
H441 cell line
Microfluidics
Liposomes
Nebulisation
Next-generation impactor
Antimicrobial efficacy

ABSTRACT

Respiratory tract infections (RTIs) are reported to be the leading cause of death worldwide. Delivery of liposomal antibiotic nano-systems via the inhalation route has drawn significant interest in RTIs treatment as it can directly target the site of infection and reduces the risk of systemic exposure and side effects. Moreover, this formulation system can improve pharmacokinetics and biodistribution and enhance the activity against intracellular pathogens. Microfluidics is an innovative manufacturing technology that can produce nanomedicines in a homogenous and scalable way. The objective of this study was to evaluate the antibiofilm efficacy of two liposomal ciprofloxacin formulations with different vesicle sizes manufactured by using a 3D-printed microfluidic chip. Each formulation was characterised in terms of size, polydispersity index, charge and encapsulation. Moreover, the aerosolisation characteristics of the liposomal formulations were investigated and compared with free ciprofloxacin solution using laser diffraction and cascade impaction methods. The in vitro drug release was tested using the dialysis bag method. Furthermore, the drug transport and drug release studies were conducted using the alveolar epithelial H441 cell line integrated next-generation impactor in vitro model. Finally, the biofilm eradication efficacy was evaluated using a dual-chamber microfluidic in vitro model. Results showed that both liposomal-loaded ciprofloxacin formulations and free ciprofloxacin solution had comparable aerosolisation characteristics and biofilm-killing efficacy. The liposomal ciprofloxacin formulation of smaller vesicle size showed significantly slower drug release in the dialysis bag technique compared to the free ciprofloxacin solution. Interestingly, liposomal ciprofloxacin formulations successfully controlled the release of the drug in the epithelial cell model and showed different drug transport profiles on H441 cell lines compared to the free ciprofloxacin solution, supporting the potential for inhaled liposomal ciprofloxacin to provide a promising treatment for respiratory infections.

1. Introduction

Respiratory infections are accountable for significant morbidity and mortality worldwide, where lower respiratory tract infections (RTIs) were reported to be the 4th leading cause of death worldwide by the World Health Organisation (WHO, 2020). The opportunistic bacterial pathogen *Pseudomonas aeruginosa* is one of the leading causes of nosocomial pulmonary infections (Ho et al., 2019). It not only causes acute infections but also contributes to debilitating chronic infections in immunocompromised patients (Park, Jeong, Lee, Kim, & Lee, 2011). *Pseudomonas aeruginosa* is the most commonly isolated pathogen from chronic lung infection sufferers such as cystic fibrosis (CF), bronchiectasis, chronic obstructive pulmonary disease (COPD), and pneumonia (Bruinenberg et al., 2010) and is considered the leading cause of

* Corresponding authors at: Macquarie Medical School, Faculty of Medicine, Health and Human Sciences, Macquarie University, Sydney, NSW 2113, Australia (H. X. Ong) and School of Mechanical Engineering, Macquarie University, 44 Waterloo Rd., Macquarie Park, Sydney, NSW, 2113, Australia (S. Cheng).
E-mail addresses: shaokoon.cheng@mq.edu.au (S. Cheng), huixin.ong@mq.edu.au (H.X. Ong).

https://doi.org/10.1016/j.ijpharm.2023.122667
Received 22 November 2022; Received in revised form 19 January 2023; Accepted 28 January 2023
Available online 2 February 2023

morbidity and mortality in this patient population (Langton Hewer & Smyth, 2017). Moreover, pulmonary *Pseudomonas aeruginosa* infections are complicated by the formation of PA biofilms in the excessive mucus produced in the respiratory tract of patients with chronic respiratory conditions, which are multi-cellular surface-attached and spatially oriented bacterial communities, composed of bacterial cells in high metabolic outer regions and low metabolic/persister cells in the central regions. Specifically, the extracellular matrix that forms part of the biofilm is a significant barrier to the penetration of antimicrobial agents.

Multiple antibiotic treatments have been used to fight RTIs, with oral intake or intravenous injection of antibiotics being the most conventional approach for drug administration. However, these approaches frequently utilise high doses which increase adverse drug effects as well as cumulative and acute toxicity. Moreover, poor bioavailability of antibiotics could lead to antibiotic resistance development (Ho et al., 2019). Delivery of an antibiotic formulation via the inhalation route is a more effective approach to treating respiratory infections. The benefits include direct targeting of the lung that allows for delivery of high local concentrations of the drugs to the target site together with a rapid onset of drug action, low systemic exposure, and consequently reduced side effects and lower risk of drug resistance emergence (Sporty, Horálková, & Ehrhardt, 2008).

Only a few antibiotics have been approved for inhaled therapy to treat pulmonary infections. Current inhalation treatments for CF, approved by the FDA are limited to tobramycin (TOBI®) and aztreonam (Cayston®) in the US, as well as polymixins (colistin and the related colomycin) in Europe. Amikacin liposome inhalation suspension (ALIS; Arikayce®) appears beneficial in both CF and non-CF populations with *M. abscessus* (MAC) lung disease (Chiron et al., 2022) and is the first therapeutic agent to be approved in the USA specifically for the treatment of MAC lung disease (Shirley, 2019). Other than ALIS, there is a lack of approved standardised antibiotic treatment for non-CF, COPD, and bronchiectasis (Cipolla, Blanchard, & Gonda, 2016). Ciprofloxacin (CIP) has the potential to be formulated as an inhaled antibiotic due to its well-established and extensively utilised broad-spectrum fluoroquinolone antibiotic that inhibits topoisomerase II and IV, which are enzymes required for bacterial replication, transcription, repair, and recombinations (Cipolla et al., 2016).

Without encapsulation, free drugs such as CIP are rapidly cleared after administration into the lung, requiring multiple daily dosing which could impact patient compliance (Hamblin, Wong, Blanchard, & Atkins, 2014; Shek, 1995; J. P. Wong et al., 2003). To improve the therapeutic efficacy of drugs, appropriate formulation strategies such as drug delivery systems (DDS) can be explored. In the field of drug delivery, nanotechnology which comprises engineered drug-loaded nanostructures and nanomaterials with diameters between 10 and 1000 nm has drawn intensive attention from the scientific community and industry (De Jong & Borm, 2008). Nanoparticles have enhanced surface area, which could increase the dissolution rate of poorly water-soluble drugs. It can also protect unstable molecules from degradation in the presence of enzymes and minimise the potential adverse effects by controlling the drug release profile and providing a physical barrier from direct contact of high drug concentration with the cellular barriers (De Jong & Borm, 2008). Liposomes are one of the most popular carrier systems in nanomedicines (Drulis-Kawa & Dorotkiewicz-Jach, 2010), with many advantages as antibiotic carriers, including improved pharmacokinetics, decreased toxicity, enhanced activity against intracellular pathogens, target selectivity, and enhanced activity against extracellular pathogens, in particular, to overcome bacterial drug resistance (Drulis-Kawa & Dorotkiewicz-Jach, 2010). Inhaled liposomal CIP formulations have been shown to improve pharmacokinetics and biodistribution by providing higher drug concentration and sustained release at the site of infection, decreasing systemic toxicity and enhancing activity against extracellular pathogens, in particular overcoming bacterial drug resistance (Cipolla et al., 2016). Thus, an inhaled liposomal formulation of CIP may be a suitable approach for treating lung infections in CF as well as in the other indications for which no inhaled antibiotics have been approved.

Thin layer evaporation or nanoprecipitation is the most widely used approach for producing liposomal formulations. However, these techniques suffer from complicated preparation steps, lack of reproducibility, controllability and low production rate (Valencia, Farokhzad, Karnik, & Langer, 2020). During the past decades, microfluidics has become an innovative manufacturing approach in the pharmaceutical and biomedical fields that enables the manipulation of nanoliters scale of fluids in submillimeter channels with control of the final formulation characteristic by tuning manufacturing parameters while producing highly homogenous nanoparticles (Martins, Torrieri, & Santos, 2018). On the other hand, 3D printing is a smart manufacturing technology that offers multiple advantages by reducing complexity and costs in developing microfluidics by rapid prototyping of personalised devices (Pranzo, Larizza, Filippini, & Percoco, 2018).

This study aimed to utilise an affordable 3D printed polypropylene-based microfluidic device that allows efficient micromixing (Tiboni et al., 2021) to produce liposomal encapsulated CIP formulations. The impact of manufacturing parameters such as flow rate, lipid composition, and antibiotic concentrations on produced formulation's physicochemical characteristics will be investigated based on the Design of Experiment (DoE). Moreover, currently, there lack of a systematic study to understand the effect of liposomal size on drug delivery performance. Thus, two formulations with different liposome sizes will be selected to investigate the impact of vesicle size on aerosolisation characteristics, drug transport kinetics, drug release profile, and biofilm-killing efficacy, in comparison with the free CIP (FC) formulation, using in vitro methodologies. Therefore, the air-interface H441 cell model integrated NGI model was used to simulate the deposition of aerosolised drugs to the distal regions of the lungs and study the drug transport kinetics and drug release profile on the epithelial cells. The air-interface biofilm model cultured using a dual-chamber microfluidic platform under the impact of aerodynamic flow was used to mimic the biofilm developed in the lung system and study the drug's antimicrobial efficacy.

2. Material and methods

2.1. Material

Ciprofloxacin hydrochloride was used as supplied (MP; biomedical Australasia Pty Limited, NSW, Australia). Polypropylene (PP) filament for 3D printing was kindly gifted from BASF (Germany). Corning® Costar® SnapwellTM with polycarbonate membrane (1.12 cm2 surface area, 0.4 μm pore size) and black 96-well plates were purchased from Sigma-Aldrich (Sydney, Australia). The H441 (HTB-174) cell line was procured from the American Type Cell Culture Collection (ATCC, Rockville, USA). P. aeruginosa (PAO1, ATCC 15692) was purchased from American Type Culture Collection (ATCC), Rockville, USA). Dulbecco's modified eagle's medium (DMEM), CelLyticTM reagent, fluorescein sodium salt, nonessential amino acids, and dialysis kit (PURX 12015) were purchased from Sigma-Aldrich. Hank's balanced salt solution (HBSS), phosphate-buffered saline (PBS), foetal bovine serum (FBS) and L-glutamine (200 mM) were purchased from Gibco, Invitrogen (Sydney, Australia). Milli-Q water was purified by reverse Osmosis (Molsheim, France). Analytical HPLC-grade solvents, including methanol, ethanol and phosphate acid, were purchased from Sigma. Centrifugal filter unit (Amicon® Ultra −0.5 mL 30 ka) was purchased from Merck Millipore.

2.2. Microfluidic production of ciprofloxacin nano-liposomes

A 3D-printed microfluidic chip with micromixing (Tiboni et al., 2021) was adopted to produce CIP nano-liposome. Briefly, the chip was printed using a fused deposition modeling 3D printer (Ultimaker 3, Ultimaker, The Netherlands) with polypropylene as a manufacturing

material. The organic phase and aqueous phase were injected into the microfluidic device via two different inlets to obtain a passive micromixing by a "zigzag" bas-relief channel. The chip was connected to two syringe pumps (Chemyx Fusion 200, Chemyx Inc., USA) through polyethylene tubing. A precise amount of hydrogenated soy phosphatidylcholine (HSPC) and cholesterol (CHOE) (3:1: w/w) dissolved in ethanol was pumped against CIP aqueous solution at controlled flow rates, and the samples were collected from the outlet of the chip. The organic solvent was evaporated under a stream of nitrogen and solvent traces were removed by keeping the liposomal formulation under vacuum overnight (Trotta, Peira, Debernardi, & Gallarate, 2002). The size of liposomes could be altered by manipulating excipients concentration, drug loading concentration, and total flow rate (TFR). A Design of Experiment (DoE) approach was applied to evaluate the parameters affecting the liposomal characteristics during microfluidics manufacturing. Briefly, the Box-Behnken statistical design (BBD) (Mujtaba, Ali, & Kohli, 2014) was implemented to evaluate the effects of three independent variables, i.e., excipient concentration, TFR, and CIP loading concentration on the size, polydispersity index, Z-potential, and encapsulation efficiency. For each independent variable low, medium, and high levels were defined. The BBD design resulted in a total of 15 experiments, as reported in Table 1, combining the minimum, maximum, and intermediate independent variable values. The data analysis was processed using Matlab (MathWorks, USA) and Origin Pro 2021 (OriginLab, USA). Formulations were produced with the different parameters combinations of excipient concentrations (10, 15, and 20 mg/mL), TFR (10, 20, and 30 mL/min), CIP loading concentrations (100, 1650, and 3200 ug/mL), and defined flow rate ratio (FRR) 1:3 (ethanol: water) following the DoE analysis. All the liposomal formulations were characterised in terms of average particle size, polydispersity index (PDI), encapsulation efficiency (EE%) and Z-potential as described in section 2.3.

The application of Analysis of Variance (ANOVA) was used to select the suitable mathematical model able to correlate the input parameters (excipient concentrations, TFR, CIP loading and FRR) with the output results (particle size, PDI, EE% and Z-potential). The best mathematical model was selected by comparison of several statistical parameters including the significance of the model at the 5 % significant level (p-value < 0.05), the multiple correlation coefficient (R2), the adjusted multiple correlation coefficient (R2-adj) and the predictive R2 (R2-pred). The R2-adj is a modified version of the R2 and it increases only if the new terms of the equation improve the regression model; while the R2-pred indicates how well the regression model predicts the output results (Fukuda, Pinto, Moreira, Saviano, & Lourenço, 2018). Based on the analysis, two manufacturing conditions to produce the smallest and largest average size, respectively, with the same CIP concentration solution, were selected for the subsequent study.

2.3. Quantification of ciprofloxacin by High-Performance liquid chromatography (HPLC)

The Shimadzu Prominence UFLC system (Shimadzu Corporation, Kyoto, Japan) was used to quantify ciprofloxacin. The system consisted of an SPD-20A UV–vis detector, LC-20AD liquid chromatography, SIL-20A HT Autosampler, and LabSolution software. A Luna C-18 (2) 100A column (3 μm, 150 × 4.6 mm) (Phenomenex Pty, ltd, Lane Cove, Australia) was used with chromatography conditions conducted using a mobile phase composition of methanol and 0.1 M sodium dihydrogen phosphate at a 30:70 (v/v) ratio, and pH adjusted to 3.30 with phosphoric acid. The flow rate was set to 1 mL/min and 20.0 μL of each sample was injected into the system, with the column temperature set to 40 °C and the detection wavelength of 275 nm. Linearity was obtained between 0.01 and 100 μg/mL ($R^2 > 0.999$) at a retention time of 10.5 min.

2.4. Characterisation of nano-liposomal ciprofloxacin

2.4.1. Dynamic light scattering

The average particle size (Z-average), PDI and Zeta-potential of prepared nano-liposomal CIP (NLC) formulations were measured using dynamic light scattering Malvern Zetasizer Nano ZS (Malvern, UK). The short-term stability of selected CIP-loaded liposomes was determined with respect to the changes in size, PDI, and Zeta potential. The formulations were stored at 4 °C and room temperature (22 °C) for 21 days, with the sample collected on pre-determined days.

2.4.2. Encapsulation efficiency

The encapsulation efficiency (EE%) was evaluated using a centrifugal ultrafiltration method (Wallace, Li, Nation, & Boyd, 2012). Briefly, 0.3 mL aliquot of NLC was loaded into the centrifugal filter unit (30 kDa) and centrifuged at 22 °C for 45 min at 7,500 *g* using a centrifuge. The relatively low centrifugal force may minimize the potential for particle deformation and therefore will not compromise the particle integrity (Wallace, Li, Nation, & Boyd, 2012). At 7,500 *g*, the free drug solution in the preparation (the filtrate) was completely filtered through after 45 min centrifugation. The concentrates (pure liposomes) were dissolved in methanol and analysed by HPLC to evaluate the content of ciprofloxacin encapsulated in the liposomes. The content of the free drug was also analysed by HPLC from the filtrates. The EE% was calculated using the following equation:

$$Encapuslation\ Efficiency(\%) = \frac{Encapuslated\ drug\ mass}{Encapslated\ mass + Free\ drug\ mass} \times 100\% \quad (1)$$

Table 1
Input parameters and observed responses in Box-Behnken design.

Run	Excipient (mg/mL)	Drug loading (μg/mL)	TFR (mL/min)	Size (nm)	PDI	Z-Potential (mV)	EE (%)
1	10	100	20	142	0.32	−20.37	36.6
2	15	100	10	182.9	0.35	−23.2	34.91
3	20	100	20	186.1	0.38	−24.37	40.99
4	10	1650	30	113.5	0.29	−34.67	41.65
5	10	1650	10	224	0.48	−22.53	39.12
6	15	1650	20	254.1	0.37	−8.62	44.15
7	15	1650	20	199.3	0.38	−16.9	47.22
8	15	1650	20	178.3	0.38	−5.85	49.61
9	20	1650	30	171.1	0.41	−35.17	46.77
10	20	1650	10	236.4	0.32	−40.67	31.77
11	15	3200	30	171.3	0.42	−20.5	46.92
12	20	3200	20	234	0.42	−24.67	47.2
13	10	100	20	142	0.32	−20.37	36.6
14	15	100	10	182.9	0.35	−23.2	34.91
15	20	100	20	186.1	0.38	−24.37	40.99

2.5. Characterisation of nebulised formulations

Nebulisation of the CIP formulations were performed using the PARI LC Sprint® jet nebuliser powered by the Pari Turbo Boy S compressor (Starnberg, Germany). The reservoir of the nebuliser was filled with 2 mL of respective formulations before nebulisation.

2.5.1. Laser diffraction

The aerosol size distribution of the nebulised formulation was determined by laser diffractometry using a Spraytec particle sizer, Malvern Instrument Ltd (Malvern, UK). The details of the equipment set-up have been detailed in a previous study (Ong et al., 2012). Measurements were made at ambient temperature (25 °C) with an approximate relative humidity of 30 %. The air pump was set up at a flow rate of 15 L/min and aerosol size measurements were initiated 5 s prior to nebulisation and ceased 10 s after no aerosol was detectable. The samples were analysed in six replicates. As for data analysis, detectors 1–6 were excluded to account for beam steering, and an algorithm to correct multiple scatters within the Malvern software was activated. Light transmission was maintained above 70 % for all measurements, ensuring the absence of multiple scattering and vignetting (Dumouchel, Yongyingsakthavorn, & Cousin, 2009). Median droplet size (MDS) and geometric standard deviation (GSD) were determined by averaging all data points, excluding the first and last 10 s of nebulisation.

2.5.2. Cascade impaction

Further characterisation of nebulised aerosols was performed using the next-generation impactor (NGI) (Copley Scientific, UK) at ambient temperature (25 °C) and approximate relative humidity of 30 %. Cascade impaction was calibrated to a flow rate of 15 L/min for approximately 1 min following the standards of British Pharmacopeia (Apparatus E) to mimic the tidal breathing of an adult (Pharmacopoeia, 2009). The nebuliser was fitted to a rubber adapter to obtain a sealed attachment to the United States Pharmacopoeia (USP) throat that was connected to the NGI. Selected samples (two liposomal CIP formulations with different vesicle sizes) were nebulised at a flow rate of 15 L/min for approximately 1 min. For mass recovery assay, each NGI stage cup and USP throat were oven dried at 60 °C for 10 min to evaporate the aqueous phase before cooling to ambient temperature. The components were then individually rinsed with 5 mL of 60:40 (%v/v) methanol: water for the formulations. Quantification of the CIP in these samples was achieved using the HPLC method described previously. Each formulation was tested in triplicate.

2.6. In vitro drug release test

The dialysis bags were kept overnight in PBS solution before dialysis to ensure the thorough wetting of the membrane. 1.5 mL of free drug formulation or nanoliposomal formulations (CIP concentration 1650 μg/mL) were added into the dialysis bag and then the dialysis kit was submerged in 350 mL PBS solution (PH = 7.0) and kept at 37 °C. Samples of 1 mL were collected at fixed time intervals outside of the bag and analyzed for CIP concentration by HPLC.

2.7. Deposition and evaluation of drug transport using air interface pulmonary epithelial model.

H441 cells are representative of the alveolar epithelium in the lung and can be used as an in vitro model for transport studies of distal lung epithelial barrier (Ren, Birch, & Suresh, 2016; Salomon et al., 2014). H441 alveolar cells were grown at the air–liquid interface (ALI) as described previously (Wong et al., 2022) to allow cell monolayer differentiation. Experiments were performed on day 13 from passage 65. Deposition of aerosolised formulation onto the H441 alveolar cells was performed using a modified NGI. The set-up of the apparatus is described in detail elsewhere (van Rensburg, van Zyl, & Smith, 2018; Wong et al., 2022). Briefly, the NGI assembly was modified to incorporate H441 alveolar cells grown on Snapwell insert at stage 7. A custom-made mouthpiece adapter connecting the PARI LC Sprint® nebuliser, powered by the PARI TurboBoy®S compressor, was fitted to the throat piece of the NGI. Prior to the transport study, the FC and NLC formulations were diluted to a final concentration of 1650 μg/mL with HBSS. FC of this concentration value has shown to be able to kill 99.9 % of bacteria in the 48 h-old biofilm grown on ALI using the dual-chamber microfluidic device. 2 mL of the diluted FC or NLC was introduced into the reservoir of the nebuliser. The vacuum pump was switched on for 5 s at a flow rate of 15 L/min to allow for equilibration before samples were nebulised for an additional 5 s to prevent drying of the cells. The Snapwell insert at stage 7 was immediately removed after deposition and the outer surface was wiped dry to remove any aerosol droplets adhering to the outer surface. Subsequently, the Snapwell inserts were placed in a 6-well plate with 2 mL of HBSS in the basolateral compartment. The plate with cells was then placed in a humidified incubator (37 °C and 5 % CO2). At successive time points, 200 μL were withdrawn from the basolateral chamber and replenished with an equal volume of transport medium. At the end of the experiment, cells on the surface of Snapwell inserts were washed with HBSS to quantify the amount of residual CIP remaining on top of the cell layer. CelLyticTM lysis reagent (Sigma Aldrich, Sydney, Australia) was then used to determine the amount of drug permeated into the cells via the intracellular route (Wong et al., 2022). All the samples were analysed using HPLC. The estimated amount of CIP deposited on the cell was calculated as the sum of the drug that has been transported across the epithelial cells, and the drug recovered from the surface of the cell and within the cells after the 4 h period.

Subsequently, to assess the integrity of the cell monolayers, trans-epithelial electrical resistance (TEER) and permeability coefficient of sodium fluorescein across the air interface H441 epithelial cells were evaluated prior to and after the transport study. The TEER values were measured with an EVOM Voltohmmeter (World Precision Instruments, Sarasota, FL, USA) equipped with STX-2-electrodes (Ong, Traini, Bebawy, & Young, 2011; Wong et al., 2022). The TEER ($\Omega.cm^2$) values of samples were calculated using the following equation (van Rensburg et al., 2018; Wong et al., 2022):

$$\mathrm{TEER} = (R_{\mathrm{TEER}} - R_{\mathrm{Blank}}) \times A_{\mathrm{membrane}} \quad (2)$$

where R_{Blank} (Ω) is the resistance of the membrane without a cell layer and $A_{membrane}$ is the membrane surface area of the Snapwell inserts.

As for the permeability coefficient of sodium fluorescein, an impaction study was carried out as outlined in Section 2.7. After drug deposition, the Snapwell inserts were placed in a 6-well plate, where the cells were maintained in an HBSS medium (2 mL) for a further 4 h within the incubator at 37 °C. Then, 200 μL of warm sodium fluorescein (2.5 mg/mL; pre-dissolved in the HBSS transport medium) was added to the apical side of the Snapwell inserts. The permeability experiment was performed at 37 °C in the incubator for over 60 min. At pre-determined time intervals, 200 μL of samples were withdrawn from the basolateral chamber of the Snapwell inserts. After the withdrawal of each sample, an equal volume of fresh pre-warmed HBSS was added to maintain a constant volume in the basal compartment. As negative controls, Snapwell inserts with ALI cultured H441cell layer not exposed to drug deposition were used. The fluorescence intensity of sodium fluorescein was detected using a SpectraMax M2 plate reader (Molecular Devices, USA) at excitation λ of 485 nm and emission λ of 538 nm. A linear calibration curve (R2 = 0.999) was obtained between 0.00625 and 12.5 μg/mL concentrations. The apparent permeability coefficient (Papp, cm/s) was calculated using the following equation (Gholizadeh et al., 2021):

$$P_{app} = \frac{dQ}{dt \bullet C_0 \bullet A} \quad (3)$$

where dQ/dt (μg/s) is the mass flux of the Na-Flu, C_0 (μg/mL) is the

initial concentration of Flu-Na in the donor compartment, and A (cm^2) is the membrane area of the Snapwell inserts.

2.8. In vitro biofilm eradication efficacy evaluation

The antimicrobial efficacy of FC and NLC formulations were tested in vitro on 48 h-old biofilm developed at the ALI cultured under dynamic conditions (Uair = 30 mL/min, Umedia = 50 μL/h) in a novel dual-chamber microfluidic device developed previously (Zhang, Silva, Young, et al., 2022). The set-up procedures of the device and the protocol for biofilm culture and antibiotic susceptibility tests were described in detail elsewhere (Zhang, Silva, Young, et al., 2022). The FC and NLC formulations were diluted to a final concentration of 1650 μg/mL with sterilised Milli-Q water. Approximately 100 μL solution was injected into the top chamber, and the 48 h-old biofilm was exposed to antibiotics for 6 h at 37 °C. While the biofilm was exposed to the antibiotic, PBS was continuously infused into the bottom chamber at a flow rate of 100 μL/h. The viable cell number was determined after treatment using the colony-forming unit (CFU) count method described previously (Zhang, Silva, Traini, et al., 2022). The test was repeated six times (2 technical replicates × 3 biological replicates) for each formulation.

2.9. Statistical analysis

All results are expressed as mean ± standard deviation of at least three separate determinants. One-way ANOVA or unpaired 2-tailed t-tests were performed to determine significance (which was quoted at the level of $p < 0.05$) between treatment groups and control.

3. Results and discussion

3.1. Nano-liposome manufacture

Using the 3D-printed zig-zag microfluidic device, the TFR, loading excipient concentration, and loading drug concentration are potential factors that could significantly affect the liposomes' characteristics (Tiboni et al., 2021). To investigate the impact of these three factors, an experimental matrix (Table 1) provided by the DoE was carried out. The size, PDI, Zeta potential, and encapsulation efficiency (EE%) were measured for all the formulations and shown in Table 1.

All the results observed for the 15 formulations were initially fitted with the non-linear quadratic model. After that, for each result, the mathematical model was refined by eliminating the non-significant terms of the non-linear quadratic model, which are terms with a p-value higher than 0.05 (Table S1). In Table 2, the statistical parameters related to the mathematical models used for the fitting of each result are shown. The non-linear quadratic model is not significant for the size and the EE% (p-value > 0.05). The refined mathematical models proposed for these two output responses are characterised by a p-value lower than 0.05 which makes them significative fitting models. On the other hand, the non-linear quadratic model is significative for PDI and Z-potential (p-value < 0.05); nevertheless, some terms of the quadratic equation are not significative (Table S1). Compared to the non-linear quadratic model, the refined ones proposed for PDI, and Z-potential showed comparable R^2-adj and a higher R^2-pred, thereby fitting models better than the quadratic one.

Each output response was fitted with the appropriate refined mathematical model and the 3D surface plots describing the effects of the input parameters on the output responses are shown in Fig. 1. As observed, the size of nanoparticles slightly increases with increasing the excipient amount and by increasing the drug loading; while it decreases with increasing the TFR (Fig. 1a, 1b). The PDI is not influenced by the excipient amount and TFR, but it increases with increasing the drug loading (Fig. 1c, 1d). The Z-potential increases with the excipient increase until about 15 mg/mL and TFR increases until 20 mL/min; while it decreases for further increase of excipient amount and TFR (Fig. 1e, 1f). Finally, the EE% is not influenced by the excipient amount; it increases with increasing the TFR and the drug loading until 1650 μg/mL; after which it decreases for higher drug loading (Fig. 1g, 1 h). However, the maximum EE% is still below 50 %, which could be due to the passive loading technique used. Previous studies have also reported low encapsulation efficacy with the passive loading approach compared to the active loading techniques (Maja, Željko, & Mateja, 2020).

To study the impact of vesicle size on drug performance, two formulations with very different sizes with the same CIP loading concentration were selected. Based on the DoE analysis, the smallest and the largest vesicle size was produced under the condition of TFR = 30 mL/min, excipient concentration = 10 mg/mL (Run 4) and TFR = 10 mL/min, excipient concentration = 20 mg/mL (Run 10), respectively, with a CIP loading concentration of 1650 μg/mL. Under these conditions, the predicted size of the smallest and largest vesicles was 134 nm (PDI = 0.317) and 225.4 nm (PDI = 0.317). The predicted Z-potential for the smallest vesicles was −34 ± 4 mV and the predicted EE% was about 48 ± 6 %. On the other hand, the predicted Z-potential for the largest vesicles was −41 ± 4 mV and the predicted EE% was 37 ± 6 %.

3.2. Stability of liposomal ciprofloxacin

The short-term stability of selected nano-liposomal ciprofloxacin formulations with small vesicle (NLC-S) and large vesicle (NLC-L), was investigated at both room temperature (22 °C) (Fig. 2 A-C) and 4 °C (Fig. 2 D-F) for 21 days to ensure that the NLCs remained stable throughout the study. It can be observed that NLC-S is more stable than NLC-L, regardless of storage temperature, over the experimental period, with the size maintaining at approximately 105 nm, PDI < 0.4 and Zeta potential around −10 mV. Conversely, NLC-L was less stable, with larger fluctuations in size and Zeta potential observed. When stored at room temperature, the detected size of NLC-L was stable for the initial seven days (≈250 nm); however, it increased significantly on Day 11 and Day 14. On Day 21, the measured size of NLC-L returned to its initial size (≈ 250 nm). It is hypothesised that liposome aggregates were formed in the solution on Day 11 and Day 14, and dissipated on Day 21, with the measured size of NLC-L returning to the initial size. When stored at 4 °C, a significant size change was observed on Day 21. The Zeta potential of NLC-L formulation began slowly losing negative charge from Day 14. On Day 21, the charge becomes almost neutral at 4 °C and becomes positive

Table 2
Statistical parameters related to the fitting mathematical models.

Response	Equation	R^2	R^2-Adj	R^2-pred	p-value
SIZE (nm)	$y = \sum_{i=1}^{3} a_i x_i + \sum_{ij=1}^{3} a_{ij} x_i x_j + \sum_{i=1}^{3} a_{ii} x_i^2 + y_0$ **(Non-linear quadratic model)**	0.8901	0.6923	0.6718	0.0562
PDI		0.9435	0.8418	0.1177	0.0122
Z-Potential (mV)		0.9335	0.8137	0.6688	0.0179
EE%		0.8625	0.6151	−09426	0.0913
SIZE (nm)	$y = \sum_{i=1}^{3} a_i x_i + y_0$	0.7831	0.7239	0.6642	0.0006
PDI	$Y = a_2 x_2 + a_{12} x_1 x_2 + a_{13} x_1 x_3 + y_0$	0.8696	0.8340	0.7137	<0.0001
Z-Potential (mV)	$y = a_1 x_1 + a_{13} x_1 x_3 + a_{11} x_1^2 + a_{33} x_3^2 + y_0$	0.8840	0.8376	0.7665	0.0001
EE%	$y = a_3 x_3 + a_{22} x_2^2 + y_0$	0.4421	0.3491	0.1561	0.0301

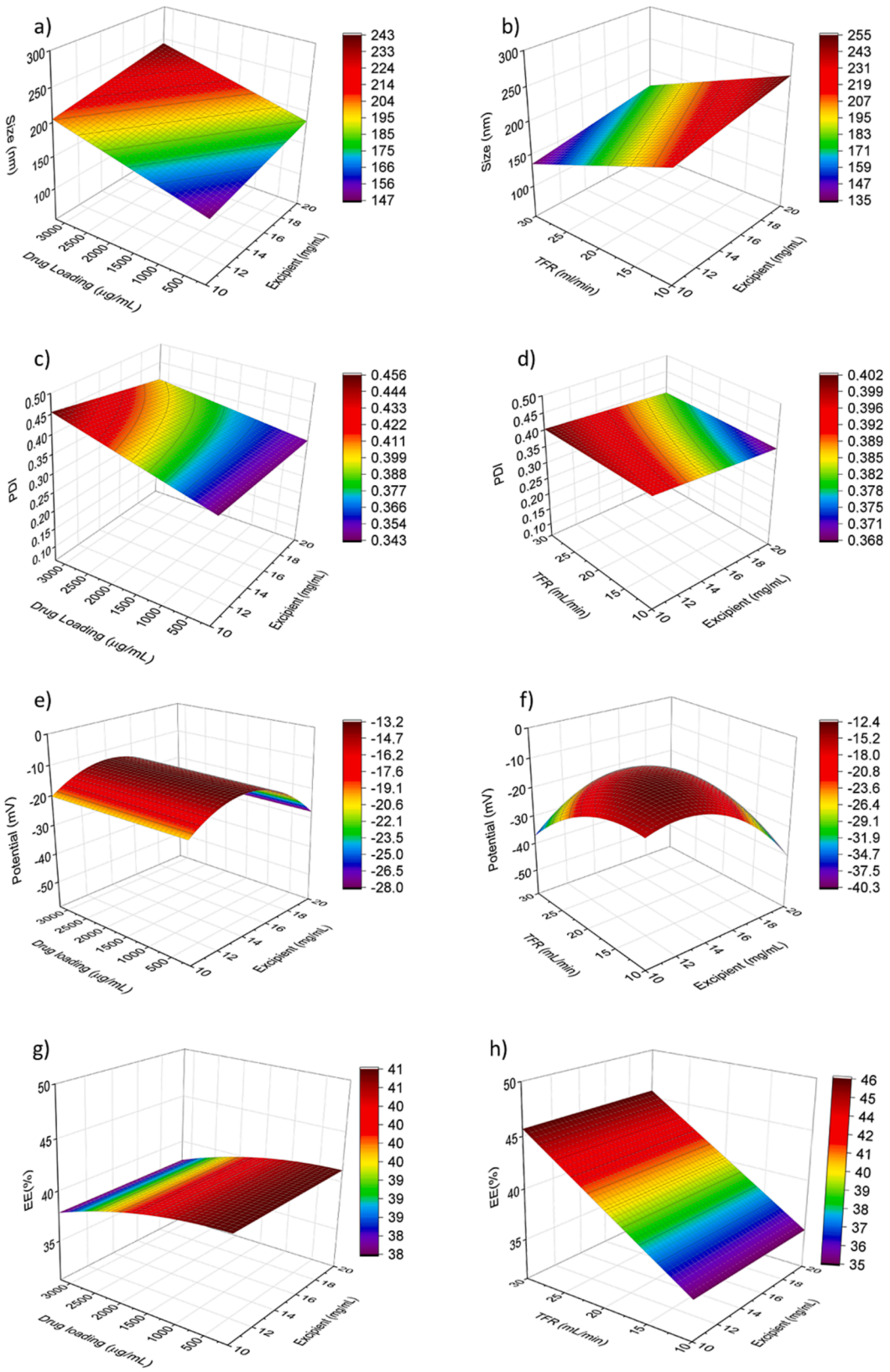

Fig. 1. 3D response surface plots: (a) size as a function of excipient concentration and drug loading; (b) size as a function of excipient and TFR; (c) PDI as a function of excipient concentration and drug loading; (d) PDI as a function of excipient concentration and TFR; (e) Z-potential as a function of excipient concentration and drug loading; (f) Z-potential as a function of excipient concentration and TFR; (g) EE% as a function of excipient concentration and drug loading; (h) EE% as a function of excipient concentration and TFR.

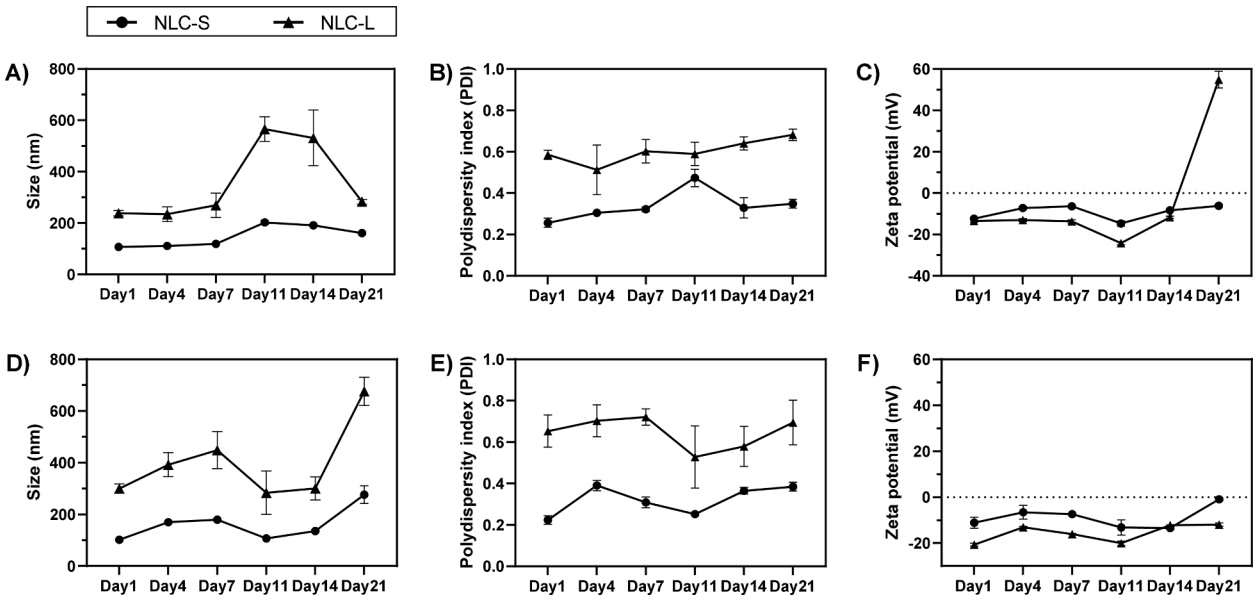

Fig. 2. The stability of selected nano-liposomal ciprofloxacin formulations (NLC-S: small vesicle size, NLC-L: large vesicle size) kept at room temperature (22 °C) (A-C) and 4 °C (D-F). Samples were tracked for 21 days with respect to size (A, D), PDI (B, E), and Zeta-potential (C, F). The results represent mean ± SD, n = 3.

(≈55 mV) at room temperature. It is hypothesised that temperature is the main factor that affects liposomes' stability since at room temperature there was an increase in charge dissipation and liposome aggregates formation. Overall, both formulations were stable and showed smaller fluctuations in terms of size, PDI and charge within 7 days at room temperature and 14 days at 4 °C storage conditions. Based on these preliminary results, the formulations produced were stored at 4 °C no longer than 14 days for subsequent studies and new batches were produced when required.

3.3. Evaluation of nebulised formulations using laser diffraction and cascade impaction

Cascade impaction has been the gold standard for assessing aerosol performance and size as recommended by regulatory bodies such as British Pharmacopeia and the United States Pharmacopeia. Laser diffraction is an established alternative to cascade impaction for size characterisation of aqueous aerosol due to the ease of operation and analysis compared with cascade impaction. However, laser diffraction has been subjected to varying data interpretation as manufacturers utilise different algorithms and orientations of detectors, leading to differences in results. In addition, laser diffraction suffers from beam steering, multiple scattering, and vignetting (Chan, Kwok, Young, Chan, & Traini, 2011; Ong et al., 2012). Hence, cascade impaction was performed in this study to validate results obtained via laser diffraction.

The characteristics of the aerosol of all the formulations generated from the nebuliser in terms of median diameter (MD), fine particle fraction (FPF), and geometric standard deviation (GSD) using laser diffraction and cascade impaction, respectively, are shown in Table 3. Data obtained from laser diffraction and cascade impaction were compared, and no significant difference (p-value > 0.05) for all formulations was observed. Therefore, cascade impaction confirmed the correlations with laser diffraction for nebuliser aerosol sizing. The previous study also (Ong et al., 2012) demonstrated that the results obtained with laser diffraction were aligned with the data obtained from cascade impaction. In addition, comparing the value of MD, FPF, and GSD, respectively, between different formulations (FC vs NLC-S, FC vs NLC-L and NLC-S vs NLC-L), showed no significant difference (p-value > 0.05). No difference between FC and NLC may be owing to the similar density and viscosity of formulations, which results in the same aerosolisation characteristics (Ong et al., 2012). Moreover, the similarity between NLC-S and NLC-L may indicate that the vesicle size difference (105 nm and 250 nm) would not affect the density and viscosity of formulations, thus showing similar aerosol performance. This was in agreement with a previous study using the same approaches that analysed the aerosol characteristics of a liposomal ciprofloxacin formulation prepared by an active loading method (Ong et al., 2012). Similar aerosol characteristics (MD = 4.70 μm; GSD = 1.94) were reported further validating the reliability of using the 3D printed microfluidic to produce liposomal formulations, which is a simpler one-step manufacturing process. However, the drawback to the method is the lower encapsulation efficiency with the EE% calculated for NLC-S and NLC-L of ≈ 31 % and 29 %, respectively.

The aerosol size distribution of the different formulations measured by laser diffraction showed that for FC, NLC-S and NLC-L, the Dv50 (the maximum particle diameter below which 50 % of the sample volume exists) was < 4.96 ± 0.04 μm, 4.48 ± 0.19 μm and 4.72 ± 0.16 μm, respectively. It is widely accepted that aerosolised particles within the

Table 3
Comparison of aerosol's median diameters generated from nebuliser collected using laser diffraction and cascade impaction of all formulations: FC, NLC-S and NLC-L (mean ± SD, n = 3).

	Free ciprofloxacin solution (FC)		Nano-liposomal ciprofloxacin small (NLC-S)		Nano-liposomal ciprofloxacin large (NLC-L)	
	Laser Diffraction	Cascade impaction	Laser Diffraction	Cascade impaction	Laser Diffraction	Cascade impaction
Median Diameter (μm)	4.96 ± 0.04	4.57 ± 0.42	4.48 ± 0.19	4.35 ± 0.22	4.72 ± 0.16	3.88 ± 0.46
GSD	2.93 ± 0.03	2.03 ± 0.06	2.68 ± 0.14	1.97 ± 0.09	2.91 ± 0.06	2.15 ± 0.10
FPF (%)	54.88 ± 0.53	54.53 ± 5.13	61.98 ± 2.89	56.80 ± 3.41	56.60 ± 1.07	61.41 ± 3.79

range of 1 ~ 5 μm would be deposited into the lower regions of the respiratory tract and will have effective therapeutic effects (Brown, Gordon, Price, & Asgharian, 2013; Labiris & Dolovich, 2003; van Rensburg et al., 2018). As presented in Fig. 3 A, the data suggests that the nebulised formulations fell within the respirable size range and possessed a uniform size distribution.

The stage deposition pattern of the nebulised formulations in the NGI is displayed in Fig. 3 B. Data are represented as the percentage of total drug deposited in the throat and at each stage of the NGI over the emitted dose. The total emitted dose is defined as the total amount of drug recovered from the throat and the stages of the NGI. It can be observed that all three formulations showed a similar distribution pattern. The FPF reflects the percentage of aerosols with aerodynamic diameter below 5 μm and provides insights into the estimated drug dose that can be delivered effectively to the lungs (Darquenne, 2012; Labiris & Dolovich, 2003). Data analysis in Table 3 demonstrated that the aerosol performance of the NLS formulation with different vesicle sizes was not significantly different (NLC-S: FPF = 56.80 ± 3.4 %; NLC-: FPF = 61.41 ± 3.79 %; p-value = 0.4561). Also, no significant differences were found between FC (FPF = 54.53 ± 5.13 %) and each NLC formulation (FC vs NLC-S: p-value = 0.4561; FC vs NLC-L: p-value = 0.1360).

3.4. In vitro drug release using the dialysis method

The drug release profile of free drug solution and nanoliposomal formulations (NLC-S and NLC-L) obtained by dialysis bag method is shown in Fig. 4. ANOVA test was conducted to compare the % drug released of the nano-liposomal formulations to the free drug solution and between NLC-S and NLC-L at each time point. Results show that the percentage of drug released from the NLC-S formulation was significantly lower compared to the free drug solution after 2 h of release. No significant difference was shown between the NLC-L formulation and free drug solution. In addition, the percentage of drug released from the NLC-S formulation was significantly lower than the NLC-L formulation after 6 h of release. It can be also seen that the drug was released slowly up to 24 h, and at the 24 h time point, 100 % and 95 % of drug was released from the free solution and the NLC-L formulation, respectively, while the NLC-S formulation only showed 80 % drug release. Nanoliposomes have previously demonstrated to control the release of encapsulated drugs, thereby leading to sustained exposure at target regions and improved efficacy. This study suggests that the size of nanoliposomal formulation could affect the rate of drug release, with the smaller vesicle size formulation having a slower drug release compared to the larger vesicle size.

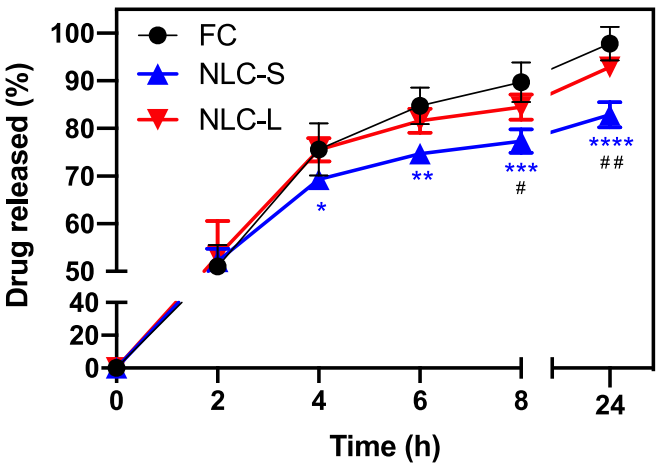

Fig. 4. Release of ciprofloxacin from free drug solution (FC) and nanoliposomal formulations for small or large vesicle size (NLC-S and NLC-L) using the dialysis bag method. * indicate the significance of difference between the free drug solution and the nanoliposomal formulation (NLC-S or NLC-L). # indicate the significance of difference between NLC-S and NLC-L. (n = 3, mean ± SD, *, p-value < 0.05; **, p-value < 0.01; ***, p-value < 0.001; ****, p-value < 0.0001).

3.5. Deposition and evaluation of drug transport using an air interface pulmonary epithelial model

The integration of epithelial cells cultured under ALI conditions into the NGI stages provides a more physiologically relevant model, in terms of a realistic aerosol deposition testing approach for drug delivery studies. The suitability of the set-up for drug transport study using this model has been previously validated by Wong et al. (Wong et al., 2022). The H441 cell line is a broadly used alveolar model that represents the deep lung region (Salomon et al., 2014). Additionally, when 15 L/min of airflow is established in the NGI assembly, it can collect drug fractions with a representative particle size of 0.98 – 1.36 μm in stage 7 for uptake by alveolar cells. Thus, in this study, the air interface culture of H441 cells was placed at stage 7 of the NGI and were used to investigate the drug transport in the alveoli region of the lung. The cell deposition and transport studies were confidently performed based on the result showing previously that FPF values are equivalent for all formulations. The release profiles over time and the transport rate of the nebulised FC and NLC formulations using the modified NGI model are shown in Fig. 5 A) and B), respectively. Drug concentrations in Fig. 5 A) are expressed in terms of the percent of total recovery throughout the experiments, and

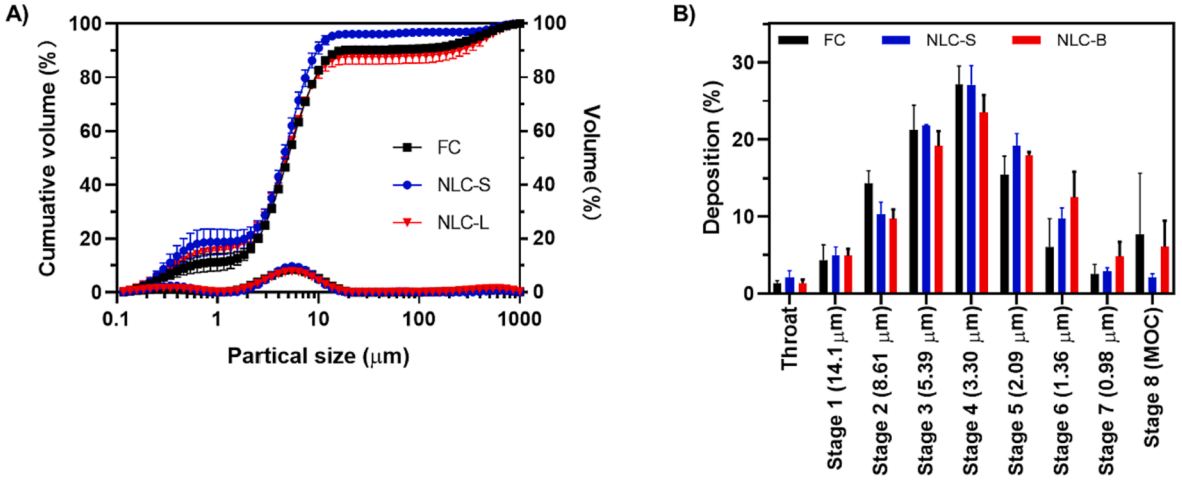

Fig. 3. A) In-line laser diffraction particle size measurement and B) BGI stage deposition data of nebulised free ciprofloxacin (FC), small size nano-liposomal ciprofloxacin (NLC-S), and large size nano-liposomal ciprofloxacin (NLC-L) formulations (n = 3, mean ± SD).

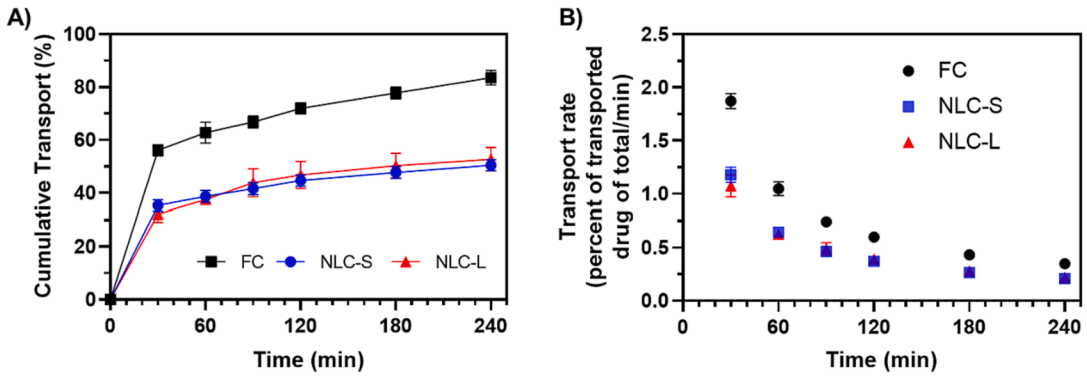

Fig. 5. Pical-basal cumulative transport a) and transport rate b) of nebulised free ciprofloxacin (FC) and nano-liposomal ciprofloxacin (NLC-S and NLC-L) on the H441 air-interface cell line (n = 3, mean ± SD).

data were plotted as the mean cumulative percentage (±standard deviation) of drug transport across the H441 cells over 4 h. The total amount of ciprofloxacin deposited onto the H441 cells from all the formulations was equivalent, with CIP recovery from the FC formulation of 3.20 ± 0.19 μg, NLC-S formulation of 5.81 ± 0.18 μg, and NLC-L formulation of 6.10 ± 0.67 μg deposited on the cells. Overall, the transport of CIP follows a two-phase profile with the initial 30 min showing a burst release profile that correlates to the rapid permeability of free CIP component of the formulation. This is then followed by the slow release of CIP from liposomes was well controlled with 50 % of the drug being transported across the epithelium over 4 h. In comparison, FCI showed > 80 % of the drug transported over the same period. The drug transport rate of FC formulation is 1.5 times faster than that of NLC formulations (Fig. 5 B). This might indicate that unlike FC diffusing to the basolateral directly through cell layers, the CIP is slowly released from the liposomes into the surrounding airway surface liquid and subsequently diffuses into the surrounding epithelial lining fluid before being transported across the epithelium. The slow-release formulation allows for less frequent administration which could significantly reduce the burden of therapy for patients (Ong et al., 2012). In addition, for all the formulations, the transport rate reduced with time. This may be because as the drug accumulated in the basolateral chamber, the driving force induced by the concentration difference between the apical chamber and basolateral chamber reduced, resulting in a reduced transport rate.

The distribution of CIP in the cell model after the transport study is shown in Fig. 6. The average total drug deposited on Snapwell inserts placed at stage 7 of NGI was 3.42 ± 0.19 μg, 6.01 ± 0.17 μg, and 5.81 ± 0.67 μg for FC, NLC-S and NLC-L, respectively. Drug concentration in each compartment is expressed in terms of the percentage of total recovery. It shows that after 4 h, due to the higher availability of free CIP in the surrounding epithelia lining fluid from FC formulation, most of the drug (>80 %) was transported crossed the cell layer, leaving < 20 % of drug from FC formulation on the surface of the cell layer, with no drug detected within the cell. In comparison, the NLC formulations had less CIP (<50 %) being transported crossed the cell layer, ≈ 40 % of drugs were found inside cells, and ≈ 10 % of drugs remained on cells. The significant percentage of liposomal drugs (p-value < 0.0001) found inside the cells indicates that NLC formulations have the potential for dealing with intracellular infections, which can be attributed to the lipid nanoparticles that have been known to facilitate cellular penetration (Hosseini et al., 2022). The previous study of drug transport using a modified TSI model with Calu-3 cells also found that most FC drugs were transported across the cell layers. However, for the liposomal CIP for inhalation (CFI) formulation, <2% of the drug was transported across cell lines, >95 % of the CIP remained on the cells, and ≈3% drug was found inside cell lines (Ong et al., 2012). Interestingly, this study showed a significantly larger percentage of CIP being transported and remaining within the epithelial cells for both the NLC formulations. The cause for this variance could be attributed to several reasons. First, different in vitro cell models were adopted for the study where it has been reported that H441 alveolar cells have a looser tight junction than Calu-3 cells (Short et al., 2016; Tsuda, Henry, & Butler; Wong et al., 2022), which results in a leaky cell epithelium. Thus, in this study, FC formulation can pass through H441 cell layers through the paracellular route more freely with fewer drugs transported within the epithelium. Liposomes may diffuse into the cell more readily due to their interaction with the cellular membrane but are more difficult to be transported through the paracellular route. Secondly, the liposomal CIP formulation used in Ong's study had higher encapsulation efficacy (99 %) compared to the liposomal CIP formulation produced in this study using the microfluidic technique (EE% ≈ 30 %). Therefore, the slow drug release from liposomal vesicles and cell barrier effects may be more prominent for liposomal formulations without any free drug form. Also, the liposomal CIP formulation used in Ong's study was produced using an active encapsulation approach. In contrast, the CIP liposomes in this study were encapsulated passively. It has been reported that the release of drugs is likely to be faster for passively encapsulated liposomes (Webb et al., 1998). In addition, NLC formulations showed a slower rate of drug release compared to the FC formulation, similar to the drug release result obtained by the dialysis bag method (Fig. 4). However, no significant difference was observed between the NLC-S and NLC-L formulations using the in vitro air–liquid interface model of H441 cell line. The difference in results could be explained due to the different nature of

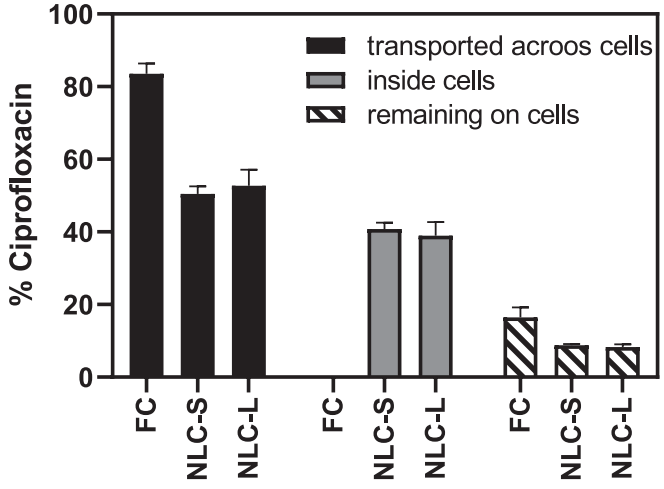

Fig. 6. Distribution of ciprofloxacin intracellularly, remaining ton the H441 epithelial cells and transported across the epithelial cells after 4 h for free ciprofloxacin and nano-liposomal ciprofloxacin (NLC-S and NLC-L) (n = 3, mean ± SD).

physical barriers for drug release between the dialysis membrane and air–liquid interface model, the latter being more physiologically relevant to the human lung. Finally, in this study, the aerosolised drug was collected on stage 7 of NGI, which has the finest droplet deposition on H441 alveolar cells that may also lead to more drugs exposed to the epithelial lining fluid (Wong et al., 2022).

To assess the impact of drug exposure on the integrity of the epithelial cells, TEER measurements were performed before and after the experiments. In addition, the paracellular permeability of the cells was also determined for the untreated and drug-exposed cells to further confirm the barrier integrity of the H441 cell monolayer. The measurements are displayed in Table 4. No significant difference was found between the TEER measured before and after drug exposure of all ciprofloxacin formulations (p-value > 0.05). The permeability of Flu-Na also showed no significant difference between control cells and drug-exposed cells (p-value > 0.05). This suggests that the deposition of the nebulised formulations did not affect the epithelial cell integrity under the conditions and timescale studied. The TEER values measured in this study were similar to previous findings (Wong et al., 2022), indicating the reproducibility and high integrity of the air interface H441 cell model.

3.6. In vitro biofilm eradication efficacy

The in vitro biofilm eradication activities of the two liposomal CIP formulations (NLC-S and NLC-L) were compared with FC solution on a 48 h-old PAO1 biofilm using a novel dual-chamber microfluidic device. The biofilms were developed at the ALI under dynamic culture conditions, which mimics the biofilm infection developed in the lung. The CIP delivered to the top chamber of the device mimics the drug deposition in the bacteria infection site in the lung, and the flow in the bottom chamber mimics the systemic flow. Results (Fig. 7) showed that after 6 h of drug exposure, FC solution (1650 μg/mL) killed > 99.9 % of bacteria compared to untreated biofilm. This is similar to the previous study's founding (Zhang, Silva, Traini, et al., 2022). NLC solutions also significantly eradicated biofilm (99.8 % and 99.7 % for NLC-S and NLC-L, respectively). However, statistical analysis showed that the difference in biofilm eradication efficacy between two NLC formulations or between NLC formulations and FC solution was not significant. In contrast, previous studies of liposomal CIP formulation demonstrated improved antimicrobial activity against Gram-negative bacteria such as *P. aeruginosa* compared to FC solution (Furneri, Fresta, Puglisi, & Tempera, 2000; Jia, Joly, & Omri, 2010; Mugabe, Halwani, Azghani, Lafrenie, & Omri, 2006; Ong et al., 2012). However, it is worth noting that these studies investigated minimum inhibitory concentration (MIC) and minimum bactericidal concentration (MBC), which are indicators of antimicrobial efficacy regarding planktonic *P. aeruginosa* bacteria rather than biofilm. It has been well known that biofilms are 100 ~ 1000 times more resistant to antibiotics compared to planktonic bacteria due to their complex 3D extracellular polymeric substance (EPS) matrix structure, and chronic lung infections are mostly related to *P. aeruginosa* biofilm (Maurice, Bedi, & Sadikot, 2018). Thus, the in vitro model used in this study is a more physiologically relevant model for testing the drug efficacy in treating bacterial infection disease in the lung system. Unlike the test for planktonic *P. aeruginosa*, no improvement in biofilm eradication was observed for CIP encapsulated in liposomes compared to FC in this study. However, based on the results from the transport study, it is reasonable to postulate that liposomes can control the release of encapsulated CIP over an extended period at the site of infection in the respiratory tract that can avoid overdosing and prevent fast systemic absorption and hence will result in better efficacy *in vivo*. In addition, biofilm resistance is primarily determined by its complex EPS matrix, which shields the bacteria from exposing to the drug directly and renders extreme resistance to antibiotics. Biofilm eradication studies using liposomal formulations with higher encapsulation efficacy and longer drug exposure time can be performed in future to assess if there is a better biofilm eradication effect.

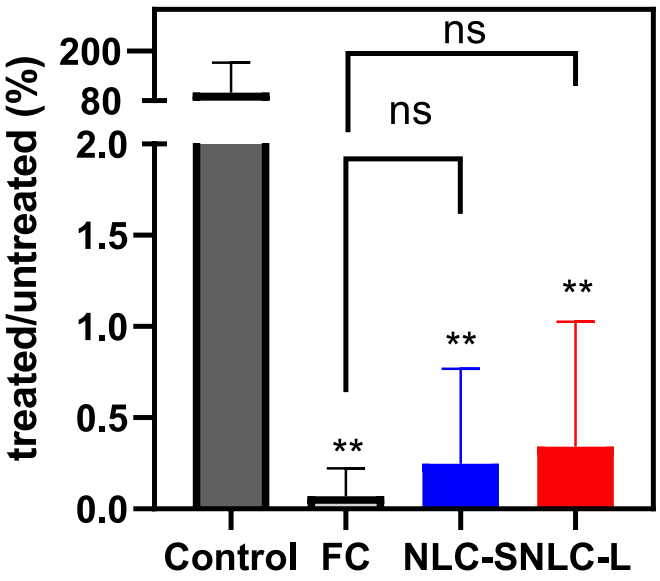

Fig. 7. Comparison of biofilm eradication effect of free ciprofloxacin (FC), nano-liposomal ciprofloxacin (NLC-S and NLC-L) for 6 h exposure on 48 h-old biofilms cultured on ALI. The significant difference is shown for the indicated comparison (N = 6, mean ± SD, **, p-value < 0.01, ns, no statistical significance).

Table 4
TEER ($\Omega \cdot cm^2$) and of H441 cell layers before formulations deposition and after 4 h transport and the apparent permeability coefficient (P_{app}, cm/s) of control cell layers and drug exposed cell layers (n = 3, mean ± SD).

TEER measurement				
		FC	NLC-S	NLC-L
TEER (Ω cm^2)	Before	449.9 ± 11.6	461.0 ± 23.9	390.1 ± 39.2
	After	449.9 ± 13.2	330.4 ± 58.5	361.2 ± 14.8
Permeability measurement				
	Control	FC	NLC-S	NLC-L
P_{app} (cm/s)	3.0 1 ± 0.23	3.77 ± 0.08	2.51 ± 0.16	2.44 ± 0.18

4. Conclusion

Liposomal formulations have the potential to improve pharmacokinetics and biodistribution, and inhalation administration could provide a promising new treatment for pulmonary infections with reduced systemic side effects and antibiotic resistance. In the present study, CIP-encapsulated liposomes of different sizes were successfully produced using a novel 3D-printed microfluidic chip with high reproducibility and homogenous size distribution. The integration of H441 epithelial cells cultured under ALI conditions into the NGI stage helped to elucidate the underlying mechanism by which the formulation interacts with the airway epithelium and mucus at the cellular level. This study has demonstrated that the liposomal formulation mediated a sustained release at the respiratory epithelium but did not show enhanced anti-biofilm activity against P. aeruginosa biofilm developed on the ALI. Furthermore, the size of the liposomes showed no significant impact in terms of aerosolisation characteristics and antimicrobial activity but showed an impact on the drug release rate, with the smaller liposomes having a slower drug release. Future studies will focus on improving the encapsulation efficacy of formulation using the 3D-printed microfluidic technique and refine the in vitro models to be more physiologically relevant.

Author contributions

The project was conceptualised by Y. Z. and H.X. O.. The 3D-printed microfluidic device was provided by M. T. and L.C.. The DoE was performed by A.A.. Experiments conduction and data analysis were performed by Y. Z. with advice and supervision by all co-authors. The manuscript was written by the first author with review and editing from S. C., H.X. O., Y. Z, D. T., M. T. and L. C.

CRediT authorship contribution statement

Ye Zhang: Conceptualization, Methodology, Investigation, Formal analysis, Validation, Writing – original draft. **Chun Yuen Jerry Wong:** Investigation, Methodology. **Hanieh Gholizadeh:** Investigation, Methodology. **Annalisa Aluigi:** Investigation, Formal analysis, Writing – review & editing. **Mattia Tiboni:** Conceptualization, Methodology, Writing – review & editing. **Luca Casettari:** Conceptualization, Methodology, Writing – review & editing. **Paul Young:** Writing – review & editing. **Daniela Traini:** Writing – review & editing, Supervision. **Ming Li:** Writing – review & editing. **Shaokoon Cheng:** Writing – review & editing, Supervision. **Hui Xin Ong:** Writing – review & editing, Supervision, Conceptualization.

Declaration of Competing Interest

The authors declare that they have no known competing financial interests or personal relationships that could have appeared to influence the work reported in this paper.

Data availability

Data will be made available on request.

Acknowledgment

This study supported Macquarie University Research Excellence Scholarship. Traini is currently funded by an NHMRC Investigator grant.

Disclosure Statement

No potential conflict of interest was reported by the authors.

Data Availability Statements

The datasets generated during and/or analysed during the current study are available from the corresponding author upon reasonable request.

Appendix A. Supplementary data

Supplementary data to this article can be found online at https://doi.org/10.1016/j.ijpharm.2023.122667.

References

Brown, J.S., Gordon, T., Price, O., Asgharian, B., 2013. Thoracic and respirable particle definitions for human health risk assessment. Part. Fibre Toxicol. 10 (1), 12. https://doi.org/10.1186/1743-8977-10-12.

Bruinenberg, P., Blanchard, J. D., Cipolla, D. C., Dayton, F., Mudumba, S., & Gonda, I. 2010. Inhaled liposomal ciprofloxacin: once a day management of respiratory infections. Paper presented at the Respiratory drug delivery.

Chan, J.G., Kwok, P.C., Young, P.M., Chan, H.K., Traini, D., 2011. Mannitol delivery by vibrating mesh nebulisation for enhancing mucociliary clearance. J. Pharm. Sci. 100 (7), 2693–2702. https://doi.org/10.1002/jps.22494.

Chiron, R., Hoefsloot, W., Van Ingen, J., Marchandin, H., Kremer, L., Morisse-Pradier, H., Catherinot, E., 2022. Amikacin Liposomal Inhalation Suspension (ALIS) in the treatment of Mycobacterium abscessus lung infection: a French observational experience. Open Forum Infect. Dis. https://doi.org/10.1093/ofid/ofac465.

Cipolla, D., Blanchard, J., Gonda, I., 2016. Development of liposomal ciprofloxacin to treat lung infections. Pharmaceutics 8 (1), 6. https://doi.org/10.3390/pharmaceutics8010006.

Darquenne, C., 2012. Aerosol Deposition in Health and Disease. J. Aerosol Med. Pulm. Drug Deliv. 25 (3), 140–147. https://doi.org/10.1089/jamp.2011.0916.

De Jong, W.H., Borm, P.J., 2008. Drug delivery and nanoparticles:applications and hazards. Int. J. Nanomed. 3 (2), 133–149. https://doi.org/10.2147/ijn.s596.

Drulis-Kawa, Z., Dorotkiewicz-Jach, A., 2010. Liposomes as delivery systems for antibiotics. Int. J. Pharm. 387 (1–2), 187–198. https://doi.org/10.1016/j.ijpharm.2009.11.033.

Dumouchel, C., Yongyingsakthavorn, P., Cousin, J., 2009. Light multiple scattering correction of laser-diffraction spray drop-size distribution measurements. Int. J. Multiph. Flow 35 (3), 277–287.

Fukuda, I., Pinto, C., Moreira, C., Saviano, A., Lourenço, F., 2018. Design of Experiments (DoE) applied to Pharmaceutical and Analytical Quality by Design (QbD). Braz. J. Pharm. Sci. 54 https://doi.org/10.1590/s2175-97902018000001006.

Furneri, P.M., Fresta, M., Puglisi, G., Tempera, G., 2000. Ofloxacin-loaded liposomes: in vitro activity and drug accumulation in bacteria. Antimicrob Agents Chemother 44 (9), 2458–2464. https://doi.org/10.1128/aac.44.9.2458-2464.2000.

Ho, D.-K., Nichols, B.L.B., Edgar, K.J., Murgia, X., Loretz, B., Lehr, C.-M., 2019. Challenges and strategies in drug delivery systems for treatment of pulmonary infections. Eur. J. Pharm. Biopharm. 144, 110–124. https://doi.org/10.1016/j.ejpb.2019.09.002.

Hosseini, S. M., Taheri, M., Nouri, F., Farmani, A., Moez, N. M., & Arabestani, M. R. 2022. Nano drug delivery in intracellular bacterial infection treatments. Biomedicine & pharmacotherapy, 146, 112609-112609. doi:10.1016/j.biopha.2021.112609.

Jia, Y., Joly, H., Omri, A., 2010. Characterization of the interaction between liposomal formulations and Pseudomonas aeruginosa. J. Liposome Res. 20 (2), 134–146. https://doi.org/10.3109/08982100903218892.

Labiris, N.R., Dolovich, M.B., 2003. Pulmonary drug delivery. Part I: Physiological factors affecting therapeutic effectiveness of aerosolized medications. Br. J. Clin. Pharmacol. 56 (6), 588–599. https://doi.org/10.1046/j.1365-2125.2003.01892.

Langton Hewer, S.C., Smyth, A.R., 2017. Antibiotic strategies for eradicating *Pseudomonas aeruginosa* in people with cystic fibrosis. Cochrane Database Syst. Rev. 4 (4), Cd004197. https://doi.org/10.1002/14651858.CD004197.pub5.

Maja, L., Željko, K., Mateja, P., 2020. Sustainable technologies for liposome preparation. J. Supercrit. Fluids 165, 104984. https://doi.org/10.1016/j.supflu.2020.104984.

Martins, J.P., Torrieri, G., Santos, H.A., 2018. The importance of microfluidics for the preparation of nanoparticles as advanced drug delivery systems. Expert Opin. Drug Deliv. 15 (5), 469–479. https://doi.org/10.1080/17425247.2018.1446936.

Maurice, N.M., Bedi, B., Sadikot, R.T., 2018. *Pseudomonas aeruginosa* biofilms: Host response and clinical implications in lung infections. Am. J. Respir. Cell Mol. Biol. 58 (4), 428–439. https://doi.org/10.1165/rcmb.2017-0321TR.

Mugabe, C., Halwani, M., Azghani, A.O., Lafrenie, R.M., Omri, A., 2006. Mechanism of enhanced activity of liposome-entrapped aminoglycosides against resistant strains of Pseudomonas aeruginosa. Antimicrob Agents Chemother 50 (6), 2016–2022. https://doi.org/10.1128/aac.01547-05.

Mujtaba, A., Ali, M., Kohli, K., 2014. Formulation of extended release cefpodoxime proxetil chitosan–alginate beads using quality by design approach. Int. J. Biol. Macromol. 69, 420–429. https://doi.org/10.1016/j.ijbiomac.2014.05.066.

Ong, H.X., Traini, D., Bebawy, M., Young, P.M., 2011. Epithelial Profiling of Antibiotic Controlled Release Respiratory Formulations. Pharm. Res. 28 (9), 2327–2338. https://doi.org/10.1007/s11095-011-0462-1.

Ong, H.X., Traini, D., Cipolla, D., Gonda, I., Bebawy, M., Agus, H., Young, P., 2012. Liposomal nanoparticles control the uptake of ciprofloxacin across respiratory epithelia. Pharm. Res. 29 (12), 3335–3346. https://doi.org/10.1007/s11095-012-0827-0.

Park, A., Jeong, H.-H., Lee, J., Kim, K.P., Lee, C.-S., 2011. Effect of shear stress on the formation of bacterial biofilm in a microfluidic channel. BioChip J. 5 (3), 236. https://doi.org/10.1007/s13206-011-5307-9.

Pharmacopoeia, B. 2009. Consistency of formulated preparations. Apparatus C, Appendix XII C, London.

Pranzo, D., Larizza, P., Filippini, D., Percoco, G., 2018. Extrusion-based 3D printing of microfluidic devices for chemical and biomedical applications: a topical review. Micromachines 9 (8), 374.

Ren, H., Birch, N.P., Suresh, V., 2016. An optimised human cell culture model for alveolar epithelial transport. PLoS One 11 (10), e0165225.

Salomon, J.J., Muchitsch, V.E., Gausterer, J.C., Schwagerus, E., Huwer, H., Daum, N., Ehrhardt, C., 2014. The cell line NCI-H441 is a useful in vitro model for transport studies of human distal lung epithelial barrier. Mol. Pharm. 11 (3), 995–1006. https://doi.org/10.1021/mp4006535.

Shirley, M., 2019. Amikacin liposome inhalation suspension: a review in *Mycobacterium avium* complex lung disease. Drugs 79 (5), 555–562. https://doi.org/10.1007/s40265-019-01095-z.

Short, K.R., Kasper, J., van der Aa, S., Andeweg, A.C., Zaaraoui-Boutahar, F., Goeijenbier, M., et al., 2016. Influenza virus damages the alveolar barrier by disrupting epithelial cell tight junctions. Eur. Respir. J. 47 (3), 954–966. https://doi.org/10.1183/13993003.01282-2015.

Sporty, J.L., Horálková, L., Ehrhardt, C., 2008. In vitro cell culture models for the assessment of pulmonary drug disposition. Expert Opin. Drug Metab. Toxicol. 4 (4), 333–345. https://doi.org/10.1517/17425255.4.4.333.

Tiboni, M., Tiboni, M., Pierro, A., Del Papa, M., Sparaventi, S., Cespi, M., Casettari, L., 2021. Microfluidics for nanomedicines manufacturing: An affordable and low-cost 3D printing approach. Int. J. Pharm. 599, 120464 https://doi.org/10.1016/j.ijpharm.2021.120464.

Trotta, M., Peira, E., Debernardi, F., Gallarate, M., 2002. Elastic liposomes for skin delivery of dipotassium glycyrrhizinate. Int. J. Pharm. 241 (2), 319–327. https://doi.org/10.1016/s0378-5173(02)00266-1.

Tsuda, A., Henry, F. S., & Butler, J. P. Particle Transport and Deposition: Basic Physics of Particle Kinetics. In: Comprehensive Physiology (pp. 1437-1471).

Valencia, P.M., Farokhzad, O.C., Karnik, R., Langer, R., 2020. Microfluidic technologies for accelerating the clinical translation of nanoparticles. Nano-Enabled Medical Applications 93–112.

van Rensburg, L., van Zyl, J.M., Smith, J., 2018. Deposition and transport of linezolid mediated by a synthetic surfactant Synsurf ® within a pressurized metered dose inhaler: a Calu-3 model. Drug Des. Devel. Ther. 12, 1107–1118. https://doi.org/10.2147/DDDT.S147035.

Wallace, S.J., Li, J., Nation, R.L., Boyd, B.J., 2012. Drug release from nanomedicines: Selection of appropriate encapsulation and release methodology. Drug Deliv. Transl. Res. 2 (4), 284–292. https://doi.org/10.1007/s13346-012-0064-4.

Webb, M.S., Boman, N.L., Wiseman, D.J., Saxon, D., Sutton, K., Wong, K.F., Hope, M.J., 1998. Antibacterial efficacy against an in vivo Salmonella typhimurium infection model and pharmacokinetics of a liposomal ciprofloxacin formulation. Antimicrob Agents Chemother 42 (1), 45–52. https://doi.org/10.1128/aac.42.1.45.

WHO, W. H. O. 2020. The top 10 causes of death. Retrieved from https://www.who.int/news-room/fact-sheets/detail/the-top-10-causes-of-death.

Wong, C.Y.J., Cuendet, M., Spaleniak, W., Gholizadeh, H., Marasini, N., Ong, H.X., Traini, D., 2022. Validation of a cell integrated next-generation impactor to assess in vitro drug transport of physiologically relevant aerosolised particles. Int. J. Pharm. 624, 122024 https://doi.org/10.1016/j.ijpharm.2022.122024.

Zhang, Y., Silva, D.M., Traini, D., Young, P., Cheng, S., Ong, H.X., 2022a. An adaptable microreactor to investigate the influence of interfaces on Pseudomonas aeruginosa biofilm growth. Appl. Microbiol. Biotechnol. 106, 1067–1077. https://doi.org/10.1007/s00253-021-11746-5.

Zhang, Y., Silva, D.M., Young, P., Traini, D., Li, M., Ong, H.X., Cheng, S., 2022b. Understanding the effects of aerodynamic and hydrodynamic shear forces on Pseudomonas aeruginosa biofilm growth. Biotechnol. Bioeng. 119 (6), 1483–1497. https://doi.org/10.1002/bit.28077.